

See discussions, stats, and author profiles for this publication at: <https://www.researchgate.net/publication/47642248>

# Hydration Analysis of Antiviral Agent AZT by Means of DFT and MP2 Calculations

ARTICLE *in* THE JOURNAL OF PHYSICAL CHEMISTRY B · NOVEMBER 2010

Impact Factor: 3.3 · DOI: 10.1021/jp1048452 · Source: PubMed

---

CITATIONS

12

READS

45

## 2 AUTHORS, INCLUDING:



Mauricio Alcolea Palafox

Complutense University of Madrid

129 PUBLICATIONS 1,440 CITATIONS

[SEE PROFILE](#)

# Hydration Analysis of Antiviral Agent AZT by Means of DFT and MP2 Calculations

M. Alcolea Palafox\* and Jéssica Talaya

Departamento de Química-Física I, Facultad de Ciencias Químicas, Universidad Complutense, Ciudad Universitaria, Madrid-28040, Spain

Received: May 27, 2010; Revised Manuscript Received: October 1, 2010

A theoretical analysis of the effect of hydration on the molecular structure and energetics of the most stable conformers of the nucleoside analogue AZT (3'-azido-3'-deoxythymidine) was carried out. To simulate the first hydration shell, two models were considered, namely, the polarized continuum model (PCM) and the discrete model, including a variable number (from 1 to 13) of explicit water molecules surrounding the nucleoside. More than 200 cluster structures with water were analyzed by B3LYP and MP2 quantum chemical methods. In the isolated state, conformer I is the most stable by the B3LYP method, but by the MP2 method, conformer II is most stable. With nine water molecules, conformer II changes to conformer I, and this conformer I is the most stable with the further addition of water molecules. The CP-corrected formation and interaction energies for AZT and water molecules were determined. The effects of hydration on the total atomic charges and intermolecular distances were also investigated. Several general conclusions on hydrogen-bond network and involved energies are emphasized. The computed values were in good agreement with previous results for other nucleosides.

## 1. Introduction

The search for therapeutic agents against acquired immune deficiency syndrome (AIDS)<sup>1–7</sup> is of great importance. In the different strategies developed, nucleoside analogues play a crucial role in the current treatment of viral infections and cancer.<sup>8</sup> Compounds such as AZT (3'-azido-3'-deoxythymidine; zidovudine, retrovir) belong to the most effective alternative substrates of the reverse transcriptase enzyme of the human immunodeficiency virus (HIV), and they are among the NRTIs (nucleoside reverse transcriptase inhibitors). They have been approved by the U.S. Food and Drug Administration (FDA)<sup>9</sup> for clinical use in the infection caused by HIV.<sup>10</sup> NRTIs are applied alone or in combination with other medications used to treat HIV. Different antiretrovirals have been approved for use in treating HIV disease, such as AZT, 2',3'-dideoxyinosine (ddl), and 2',3'-dideoxycytidine (ddC).<sup>1–3</sup> These nucleoside analogues have no 3'-hydroxyl groups; therefore, they inhibit further growth of a viral DNA chain.

AZT was identified in 1984 as active, first against murine retroviruses and then against HIV in cell culture.<sup>1,2</sup> In 1987, the U.S. FDA approved the first antiretroviral therapy with AZT.<sup>4</sup> AZT is a potent inhibitor of HIV-1 replication and the first clinically successful drug for AIDS and AIDS-related diseases. Its use prolongs the life of HIV-infected individuals and improves their quality of life.<sup>1</sup> After its phosphorylation to the triphosphate form (AZTTP) by host cell kinases, it can compete with endogenous nucleosides to inhibit HIV-1 reverse transcriptase.<sup>4</sup> In this form, it can also act as a chain terminator by incorporation into growing strands of DNA and RNA. However, the chronic use of AZT by HIV patients can cause severe side reactions,<sup>11</sup> particularly bone marrow suppression. In addition, the evolution of virus strains resistant to AZT during therapy renders this nucleoside less effective.

To improve the efficacy of AZT, it is necessary to design new strategies and new antivirals. To design new antivirals, it is necessary to establish the relationship between the structures, conformational features or physicochemical properties, and activities of these drugs. Several studies have been carried out with this aim.<sup>12</sup> It has been reported that anti-HIV-1 activity depends on ribose conformation;<sup>13</sup> thus, differences in the conformation of the ribose ring lead to appreciable changes in the positions of the thymine ring and the C5'-OH group. On the other hand, because the nucleosides have several specific sites for forming inter- and intramolecular hydrogen bonds, their conformers depend strongly on the solvent characteristics and the experimental conditions. A full theoretical study of the conformational preferences and charge distribution within a group of molecules could provide useful information for molecular design, as well as insight into drug–target interactions.

In previous works, we have studied the D4T (3'-deoxy-2',3'-didehydro-thymidine) nucleoside analogue.<sup>14</sup> Now, a goal of the present article is a detailed analysis for the first time of all of the conformers of AZT<sup>15</sup> at the MP2 (Møller–Plesset perturbation theory of the second order) ab initio level and a study of the effects of hydration on the two most stable conformers using explicit water molecules (discrete method) and at the highest level of calculation available under the limitations of computer memory requirements. Comparisons with the thymidine (Thy) natural nucleoside were also performed.

To our knowledge, AZT has been extensively examined for antiviral properties,<sup>11,16</sup> but less structural and energetic information, obtained from theoretical studies, is available; moreover, such information has been calculated at lower levels than used in this work.<sup>2,7,12,17–20</sup> Solution conformational studies of anti-HIV nucleosides have been infrequent. Thus, the importance of the present article. The methodology applied to the hydration in the present article is commonly used for accurate research on the effects of water, and it is detailed in the next section.

\* To whom correspondence should be addressed. E-mail: alcolea@quim.ucm.es.

## 2. Calculations

Calculations were carried out using both the MP2 ab initio method and the B3LYP (Becke, three-parameter, Lee–Yang–Parr)/density functional theory (DFT) method. These methods were implemented in the Gaussian 03 program package.<sup>21</sup> The UNIX version with standard parameters of this package was run on the alpha computer of the Computational Center at University Complutense of Madrid, Spain. DFT methods provide an adequate compromise between the desired chemical accuracy and heavy demands on computer time and power. Moreover, DFT methods and in particular B3LYP have been used satisfactorily in many studies of drug design, as well as in other nucleosides and nucleic bases,<sup>14,22</sup> and they predict vibrational frequencies better than Hartree–Fock (HF) and MP2 methods.<sup>23</sup> It is well-established that weak interactions are poorly described by DFT methods. However, the hydration of uracil and their derivatives has been reasonably well modeled by DFT.<sup>22d,e</sup> For all structures, when computer requirements allowed, MP2 computations were also performed to complement the B3LYP results.

Berny optimization under the TIGHT convergence criterion was used by minimizing the energy with respect to all geometrical parameters without imposing molecular symmetry constraints. Several basis set were used, starting from 6-31G\* to 6-311++G(3df,pd), but the 6-31G\*\* set represents a compromise between accuracy and computational cost, and thus it was the basis set selected for all of the calculations.

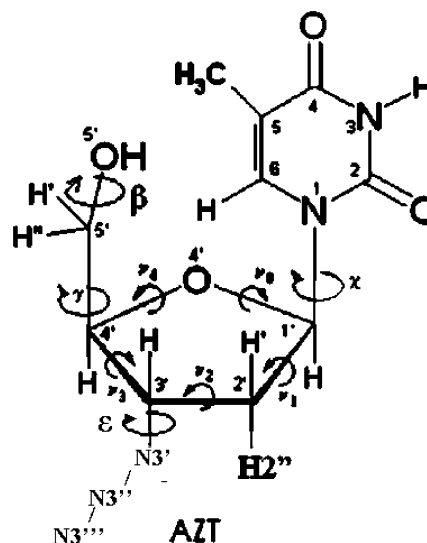
The polarized continuum model (PCM) was used with the integral equation formalism model (IEF-PCM).<sup>24,25</sup> It was applied to investigate the effect of water on the structure of AZT. Thus, all conformations were full optimized.<sup>15</sup> Atomic charges were determined with the natural bond orbital (NBO)<sup>26</sup> procedure. The NBO theory applies an interatomic orthogonalization step to establish asymmetrical atomic orbitals and thus gives relatively basis-set-independent charges compared to other methods such as Mulliken charges and their variations.

Vibrational calculations were performed on all optimized conformers (including those with PCM) to confirm that they corresponded to local minima. Harmonic frequency calculations were carried out at the same level as the respective optimization process and by the analytic evaluation of the second derivative of the energy with respect to nuclear displacement. All optimized structures showed only positive harmonic vibrations (i.e., were true local energy minima). Relative energies were obtained by adding zero-point vibrational energies (ZPEs) to the total energy. For the calculation of the ZPEs, the frequencies were unscaled.

**2.1. Definition of Conformational Angles.** There are many conformational possibilities depending on the endocyclic and exocyclic torsional angles of the molecule. Following Saenger's notation,<sup>27</sup> the atomic description of the molecule and the most important torsional angles are defined in Scheme 1.

The conformation of nucleoside is usually characterized by the following five important structural parameters: (i) the glycosylic torsional angle  $\gamma$  ( $O4'-C1'-N1-C2$ ), which determines the two orientations of the base relative to the furanose ring, denoted as the anti and syn conformations; (ii) the exocyclic torsional angle  $\gamma$  ( $C3'-C4'-C5'-O5'$ ), describing the orientation of the 5'-hydroxyl group relative to the furanose ring; (iii) the exocyclic torsional angle  $\beta$  ( $C4'-C5'-O5'-H5'$ ), defining the orientation of the hydroxyl hydrogen  $H5'$  relative to the furanose ring; (iv) the torsional angle  $\varepsilon$  ( $C2'-C3'-N3'-N3''$ ), which determines the orientation of the azide group; and (v) the furanose pucker  $P$ .

**SCHEME 1: Definition of the Exocyclic and Endocyclic Angles in the AZT Molecule**



In a crystal database of uridine analogues,<sup>28</sup> the  $\gamma$  values generally appear between  $-176^\circ$  and  $82^\circ$  (anti) with a mean value of  $-135^\circ$  and a standard deviation of  $22^\circ$ . In this database, the  $\gamma$  angle has a trimodal distribution: the main group is centered about  $60^\circ$ , and two smaller ones appear at  $180^\circ$  and  $-60^\circ$ . This distribution appears to be consistent with our results. The furanose ring is puckered significantly to minimize nonbonded interactions among the  $C5'-OH$  groups and the base substituents.<sup>2</sup> Steric hindrance probably determines changes in the puckering.

The azide group is nonlinear, and the  $\varepsilon$  angle has a preferred cis position. However, this position appears very close in energy, 0.3 kcal/mol, to the trans position reported in the crystal.<sup>28a</sup> The  $N3'-N3''-N3'''$  angle ranges from  $171.0^\circ$  to  $173.7^\circ$ , and the  $N3''-N3'-C3'-H3'$  torsion angle ranges from  $-37^\circ$  to  $-51^\circ$ . Deviation from the trans position has been correlated with an increased  $C2'$ -endo conformation of the furanose ring.<sup>28a</sup>

**2.2. Simulation of Hydration.** The hydration effects can be simulated theoretically by two procedures.<sup>29</sup>

(i) The first type of procedure is discrete methods (DMs) including a sufficient number of explicit water molecules surrounding the compound.<sup>30</sup> These water molecules are treated explicitly, providing a description of both the microscopic structure of the solvent and specific solute–solvent interactions. A selected number of solvent configurations are included in the quantum-mechanical description of the system. Unfortunately, both the large number of solvent molecules required to mimic a dilute solution and the computational cost of quantum-mechanical calculations<sup>31</sup> limit the applicability of DMs. In the present work, this method was used with up to 13 explicit water molecules surrounding the nucleoside. Vibrational frequency calculations were performed on all optimized hydration clusters to verify that they corresponded to local minimum structures.

(ii) Second, a continuum model<sup>32</sup> can be used. Such models have a solid theoretical ground and are used mostly today owing to their simplicity and lower computational time requirements. In the present work, the conformers corresponding to real minima appear markedly reduced with this model as compared to those in the isolated state.

From a theoretical point of view, a DM might be preferred, provided that the size of the considered complex is not too large. In this work, this procedure was used with several water

**TABLE 1:** Relative Energies (kcal/mol) Calculated for the Different Conformers in Anti Orientation ( $\chi \approx -120^\circ$  to  $-150^\circ$  and  $\varepsilon \approx 70\text{--}100^\circ$ ) of AZT in an Isolated State and with the PCM, and Using the B3LYP and MP2 Levels of Theory

	B3LYP/6-31G** + ZPE			B3LYP/6-31G** (PCM) + ZPE			MP2/6-31G**			B3LYP/6-311++G(3df,pd)
	$\gamma \approx 60^\circ$	$\gamma \approx -60^\circ$	$\gamma \approx 180^\circ$	$\gamma \approx 60^\circ$	$\gamma \approx -60^\circ$	$\gamma \approx 180^\circ$	$\gamma \approx 60^\circ$	$\gamma \approx -60^\circ$	$\gamma \approx 180^\circ$	$\gamma \approx 60^\circ$
$\beta \approx 60^\circ$	0.0 <sup>a,b</sup>	4.17	4.33	0.84 <sup>b,c</sup>	3.02 <sup>c</sup>	1.89 <sup>c</sup>	0.04 <sup>b</sup>	4.97 <sup>d</sup>	2.99 <sup>d</sup>	0.0 <sup>e</sup>
$\beta \approx -60^\circ$	1.76	2.60	2.01	0.32	1.65 <sup>c</sup>	1.29 <sup>c</sup>	1.63	—	2.56	—
$\beta \approx 180^\circ$	0.47 <sup>f</sup>	3.13	4.54	0 <sup>f,g</sup>	2.19 <sup>c</sup>	2.25 <sup>c</sup>	0 <sup>f,h</sup>	3.60 <sup>d</sup>	4.71 <sup>d</sup>	0.21

<sup>a</sup>  $-963.274176$  au. <sup>b</sup> Conformer I. <sup>c</sup> Saddle point. <sup>d</sup> With  $\chi \approx -170^\circ$  to  $-180^\circ$ . <sup>e</sup>  $-963.850132$  au. <sup>f</sup> Conformer II. <sup>g</sup>  $-963.309187$  au. <sup>h</sup>  $-960.8155679$  au. <sup>i</sup> 1 au = 627.5095 kcal/mol.

**TABLE 2:** Optimum Parameters, Torsional Angles (deg), Phase Angle of Pseudorotation  $P$  (deg), Sugar Conformation, and Dipole Moment  $\mu$  (D), Calculated in the Minima of Hydrated Conformers I and II at the B3LYP/6-31G\*\* Level (MP2/6-31G\*\* Level in Parentheses)

cluster	$\chi$	$\beta$	$\gamma$	$P^a$	sugar conformation	$\mu$
Conformer I						
isolated state	$-129.1$	68.8	61.9	31.32	${}^3T$	2.82
	( $-133.4$ )	(69.4)	(61.9)	(26.80)	${}^3E$	(3.76)
PCM	$-143.1$	92.3	59.7	23.71	${}^3E$	4.97
Conformer II						
isolated state	$-128.1$	176.5	50.2	162.89	${}^2E$	6.51
	( $-126.9$ )	(176.4)	(49.1)	(162.65)		(7.79)
PCM	$-125.8$	176.9	50.1	172.52	${}^3T$	8.88
1 H <sub>2</sub> O	$-126.9$	176.9	49.8	146.15	${}^1T$	7.26
	( $-126.3$ )	(176.5)	(48.9)	(143.19)		(8.55)
2 H <sub>2</sub> O	$-127.2$	176.8	49.8	145.16	${}^2T$	7.34
3 H <sub>2</sub> O	$-127.0$	177.0	49.9	144.89	${}^2T$	6.07
4 H <sub>2</sub> O	$-128.0$	177.7	50.3	145.09	${}^1T$	9.18
5 H <sub>2</sub> O	$-127.0$	176.7	49.9	146.23	${}^1T$	5.21
6 H <sub>2</sub> O	$-111.8$	120.9	51.6	150.32	${}^1T$	5.09
7 H <sub>2</sub> O	$-108.9$	120.8	52.1	166.06	${}^2E$	6.84
8 H <sub>2</sub> O	$-117.6$	127.8	51.3	165.99	${}^2E$	9.88
Conformer I						
9 H <sub>2</sub> O	$-79.8$	84.9	53.1	143.05	${}^1T$	3.76
10 H <sub>2</sub> O	$-93.7$	84.0	46.1	151.03	${}^1T$	4.74
11 H <sub>2</sub> O	$-98.0$	81.0	48.6	145.16	${}^1T$	5.22
12 H <sub>2</sub> O	$-101.9$	76.9	51.9	140.52	${}^2T$	4.05
13 H <sub>2</sub> O	$-101.9$	78.4	52.2	116.80	${}^0T$	5.83

<sup>a</sup>  $\text{tg}P = [(\nu_4 + \nu_1) - (\nu_3 + \nu_0)]/[2\nu_2[\sin(36) + \sin(72)]]$ . When  $\nu_2$  is negative,  $180^\circ$  is added<sup>20</sup> to the calculated value of  $P$ .

molecules, because it accounts for hydrogen bonds explicitly, and the first hydration shell can be better reproduced than by using the continuum model. Therefore, for accuracy, this procedure would be preferred.

**2.3. Interaction Energies with the Discrete Method.** The energies obtained using explicit water molecules were corrected for basis set superposition error (BSSE) by the counterpoise (CP) procedure.<sup>33</sup> The CP-corrected B-(H<sub>2</sub>O)<sub>n</sub> formation energy for the AZT molecule, the deformation energy of monomer X (X = AZT or W), the CP-corrected interaction energy between the nucleoside (B = AZT) and the water *n*-mer (W<sub>n</sub>), and the CP-corrected formation energy of a water *n*-mer (in the presence of AZT), at the geometry adopted in the BW<sub>n</sub> complex, were calculated according to the equations reproduced by us in ref 14.

### 3. Results and Discussion

**3.1. AZT in an Isolated State. 3.1.1. Conformers and Energetics.** AZT has a similar number of conformers as Thy,<sup>34</sup> because the azide group can be in three positions similarly to the O3'-H group in Thy. A full study without any restrictions was carried out:<sup>15</sup>  $\beta$  and  $\gamma$  angles appeared around  $60^\circ$ ,  $-60^\circ$ , and  $180^\circ$ , and conformers with  $\varepsilon = 70\text{--}110^\circ$  were always more stable than those with values of ca.  $180^\circ$  or  $-60^\circ$ . Variations in this  $\varepsilon$  angle did not produce significative changes in the

conformation adopted by the sugar or in the thymine moiety. By MP2, the number of stable conformers decreased by around 10%.

In general, the conformers differ very little in energy, corresponding to a global minimum<sup>15</sup> in the syn form with values by B3LYP of  $61.7^\circ$ ,  $43.6^\circ$ ,  $43.8^\circ$ , and  $107.7^\circ$  for the  $\chi$ ,  $\beta$ ,  $\gamma$ , and  $\varepsilon$  torsional angles, respectively (by MP2, the corresponding values are  $62.3^\circ$ ,  $41.6^\circ$ ,  $47.1^\circ$ , and  $91.4^\circ$ ). This result is in accordance with other DFT calculations.<sup>18,19</sup> However, X-ray data on AZT,<sup>28a,35–37</sup> as well as NMR studies,<sup>38,39</sup> have shown that the  $\chi$  angle is in the anti orientation (ca.  $-120^\circ$ ) with the geometry stabilized through the formation of intramolecular H-bonds. Moreover, a preference of the anti form for biological activity is also known.<sup>18,39,40</sup> Following these criteria, the nine conformers in the anti form in Table 1 were selected. They correspond to values of  $\chi$  ranging from  $-120^\circ$  to  $-150^\circ$  and  $\varepsilon \approx 70\text{--}100^\circ$ . The minimum (denoted as conformer I) with  $\chi = -129.1^\circ$  (Table 2) is in accordance with the X-ray value of  $-124.4^\circ$ .<sup>28a</sup> Selected optimum bond lengths and angles of this conformer I at the B3LYP and MP2 levels are included in Figure 1.

By the B3LYP method, the second most stable conformer in the anti range appears to be a C2'-endo ( ${}^2E$ ) pucker, denoted as conformer II (Figure 2 and Tables 1 and 2). However, according to the MP2 results, conformer II is more stable than conformer

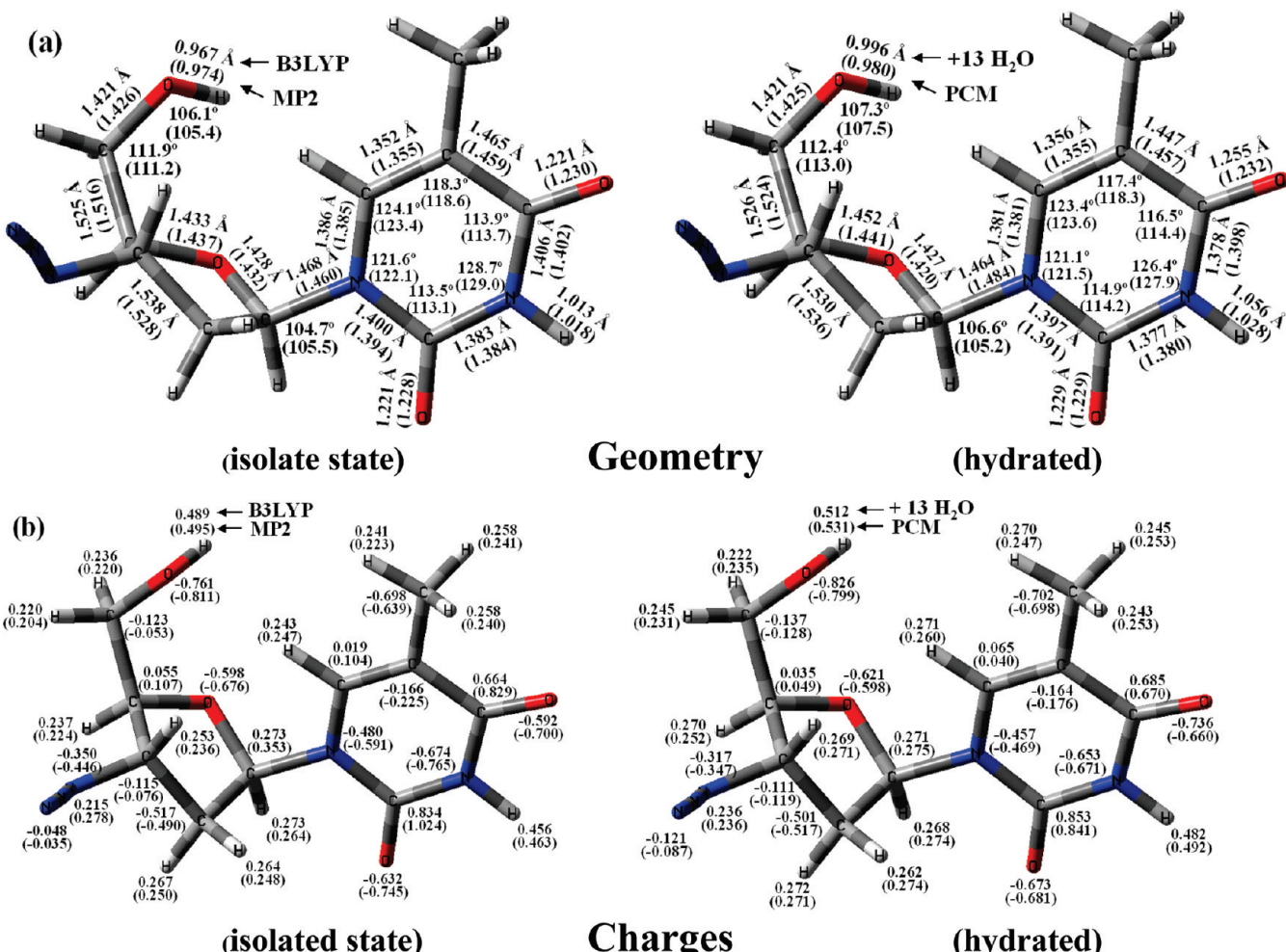


**Figure 1.** Calculated values for conformer I of AZT at the B3LYP/6-31G\*\* and MP2/6-31G\*\* (in parentheses) levels, in an isolated state and in the hydrated form: (a) optimized bond lengths and angles and (b) optimized natural atomic charges (NBO).

## CONFORMER II

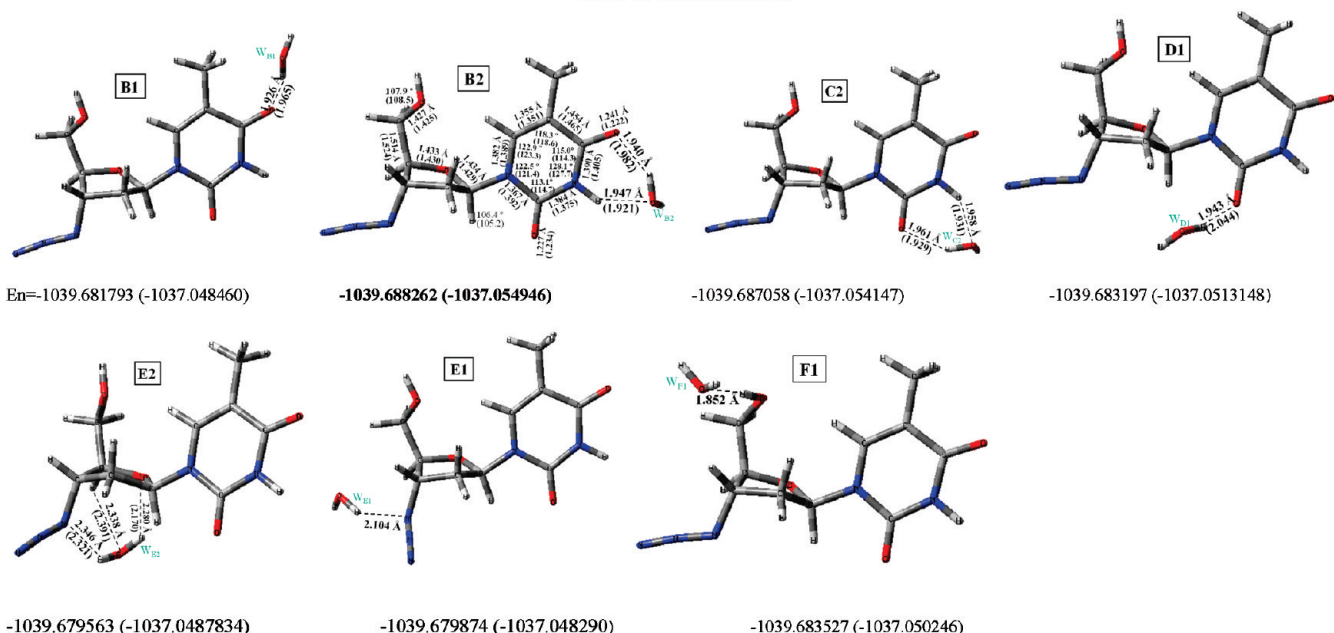


**Figure 2.** Optimum stable positions of one water molecule in the hydration of conformer II in AZT. The calculated intermolecular H-bonds correspond to the B3LYP/6-31G\*\* and MP2/6-31G\*\* (in parentheses) levels. The total energy + ZPE (in au) corresponds to the B3LYP/6-31G\*\* levels, and the value in parentheses corresponds to the MP2/6-31G\*\* level.

I, as is also the case for Thy. Thus, we discuss the results for both conformers. In conformer II, the values calculated by MP2 corresponding to  $\chi$  and  $\gamma$  ( $-126.9^\circ$  and  $49.1^\circ$ , respectively) appear closer to the X-ray values ( $-124.4^\circ$  and  $50.9^\circ$ , respectively)<sup>28a</sup> than those in conformer I. These values are also close to the expected ones for the natural nucleosides and nucleotides in biological systems<sup>27</sup> and confirm that a value of  $\gamma$  around  $45-65^\circ$  leads to the most stable forms. The difference in energy between the two conformers is small, 0.47 kcal/mol at the B3LYP level compared to 0.04 kcal/mol at the MP2 level.

**3.1.2. Thymine Moiety.** The ring of the thymine moiety has a nearly planar form, with a deviation from the plane smaller than  $3^\circ$  in the torsion angles, in agreement with the experimental results. The double bonds in the uridine ring are highly localized, and the bond lengths and angles appear to be little influenced by substitution of the methyl group at the 5-position. Through a rotation of this group, two conformers were obtained in AZT. Frequency calculations of these forms revealed that one is a first-order saddle point, whereas the other represents the global minimum<sup>15</sup> of the structure (Figure 1). The difference in energy between the two forms is very small, less than 5 cal/mol. Thus, only the global minimum conformation is discussed in the present article. The methyl group in AZT appears to be very slightly rotated, with a C4–C5–C7–H10 torsional angle of  $179.2^\circ$ . The values obtained indicate that the furanose moiety does not influence the parameters of the methyl group.

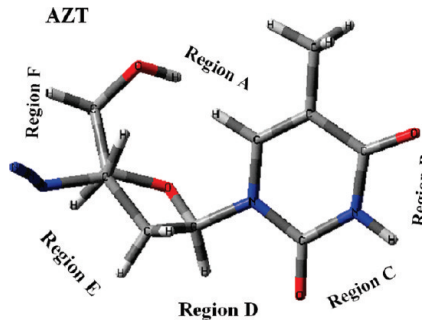
**3.1.3. Furanose Moiety.** Because of the  $sp^3$  hybridization of the C1' atom, this moiety appears out of the plane of the thymine ring, with a calculated N1–C1'–C2'–C3' torsional angle markedly different between conformers I and II, at  $102^\circ$  and  $153^\circ$ , respectively, by MP2.

The sugar is usually characterized by three structural parameters:<sup>27</sup> (i) the endocyclic torsion angles,  $\nu_0-\nu_4$ ; (ii) the pseudorotation phase angle,  $P$ ,  $tgP = [(\nu_4 + \nu_1) - (\nu_3 + \nu_0)]/[2\nu_2\{\sin(36) + \sin(72)\}]$ ; and (iii) the maximum torsional angle (degree of pucker),  $\nu_{max}$  (see Table 5, below).

In the structural analysis of AZT, two narrow ranges of  $P$  are preferred for the different conformers, namely,  $18^\circ \pm 18^\circ$  (C<sub>3</sub>-endo, “north”) and  $162^\circ \pm 18^\circ$  (C<sub>2</sub>-endo, “south”), values that are in accordance with those found in other nucleosides. Most HIV-inhibitory 3'-substituted dideoxynucleosides fall in the southern range, although, in the solid state, the common range is  $P = 10-30^\circ$ . In conformer I, the value of  $\nu_0$  ( $-5.3^\circ$  by MP2, Table 5 below) is markedly lower than those of  $\nu_1$  and  $\nu_2-\nu_4$ ,  $P = 26.8^\circ$ , with the C3' atom in an endo form, <sup>3</sup>E (Table 2). However, in conformer II, the values differ markedly,  $P = 162.65$ , <sup>2</sup>E. By contrast, the value of  $\nu_{max}$  is similar in the two conformers and in accordance with the  $35-45^\circ$  range generally observed in nucleosides. These values indicate the flexible nature of AZT, which can adopt a south conformation required for phosphorylation and subsequently switch to a north conformation for a better interaction with reverse transcriptase (RT).<sup>7,41</sup> This capacity to adopt different forms of ring pucker is a characteristic of natural nucleosides, and it is perhaps the reason why nature selected ribofuranoses and not the more rigid ribopyranoses as the building blocks of nucleic acids.<sup>41</sup>

Because of the  $sp^3$  hybridization of the C4' atom, the H<sub>2</sub>C5'-O5'H substituent appears out of the plane, with a  $\delta$  torsional angle of  $85.1^\circ$  by MP2 ( $144.6^\circ$  in conformer II). The  $\beta$  torsional angle is also of particular interest, because the phosphorylation of this group is required to carry out its

## SCHEME 2: Six Regions of H-Bond Formation with Water Molecules in AZT



biochemical activity. Because conformer II appears to be stabilized by the O5'…H6 H-bond, its value is around  $180^\circ$ .

**3.1.4. Intramolecular H-Bonds.** Although several methods have been reported for the classification of intramolecular H-bonds,<sup>42</sup> we have followed the criterion according to Desiraju et al.<sup>14,43</sup> because of the high level of our calculations. In conformer I of AZT, three weak H-bonds can be established: O2…H1' ( $2.245$  Å by MP2), O5'…H6 ( $2.452$  Å), and O4'…H5' ( $2.408$  Å). The three-center H-bond formed by the C6–H bond of the pyrimidine ring with the furanose oxygen atom and the hydroxyl of the O5'H group stabilizes the anti form.

In conformer II, only two possible weak H-bonds can be established: O2…H1' ( $2.245$  Å by MP2) and O5'…H6 ( $2.197$  Å, close to the  $2.06$  Å value for the crystal<sup>37</sup>). The O4'…H6 H-bond does not appear, as in conformer I.

In conformer I of Thy, the value of O2…H1' ( $2.254$  Å by MP2) remains similar to that in AZT, whereas O5'…H6 is very weak or almost nonexistent,  $2.837$  Å, and O4'…H6 has a long value of  $2.636$  Å. These features indicate that the structure of Thy is more open than those of D4T<sup>14</sup> and AZT and has weaker H-bonds (i.e., higher flexibility). Intramolecular H-bonds do not appear with the azide group, or with O3'–H3' of Thy.

**3.1.5. Natural NBO Atomic Charges.** The largest negative charge is on O5' and O2. It is noted that O4 and O4' atoms have similar charges (Figure 1). O2 has higher negative charge than O4. MP2 predicts a larger negative charge on the oxygen and N1 and N3 nitrogen atoms than B3LYP.

N3 has a negative charge, ca.  $0.2e$  (where  $e$  is the charge of an electron) larger than that of N1, and H5' is the hydrogen atom with the highest positive charge (i.e., it is the most reactive). The H3 hydrogen charge is only  $0.03e$  lower than that of H5'. The remaining hydrogen atoms have much less positive charge, in the range of  $0.21-0.27e$  (i.e., they are less reactive).

The charges on the nitrogens of the azide group are much lower than those on N1 and N3 (i.e., they are unreactive). On N3'' and N3''', the charge is negative, whereas that on N3'' is positive ( $0.278e$  by MP2) and close to those on the neighboring hydrogen atoms, but lower than that on H3' of the hydroxyl group of Thy ( $0.487e$ ). In Thy, the two hydroxyl groups have the same charge. The introduction of the azide group induces mainly changes in polarity and lipophilicity of the nucleoside. In general, AZT has similar charges to Thy.

**3.2. Hydration.** **3.2.1. Monohydration.** Clusters and Energies. Six regions in AZT, labeled as positions A–F, appear to be favorable for water molecules (Scheme 2). This notation is in accordance with that followed for Thy.<sup>14b</sup> Figures 2 and 3 correspond to conformers II and I, respectively. In these figures, the water molecule is placed in all possible stable positions,

## CONFORMER I

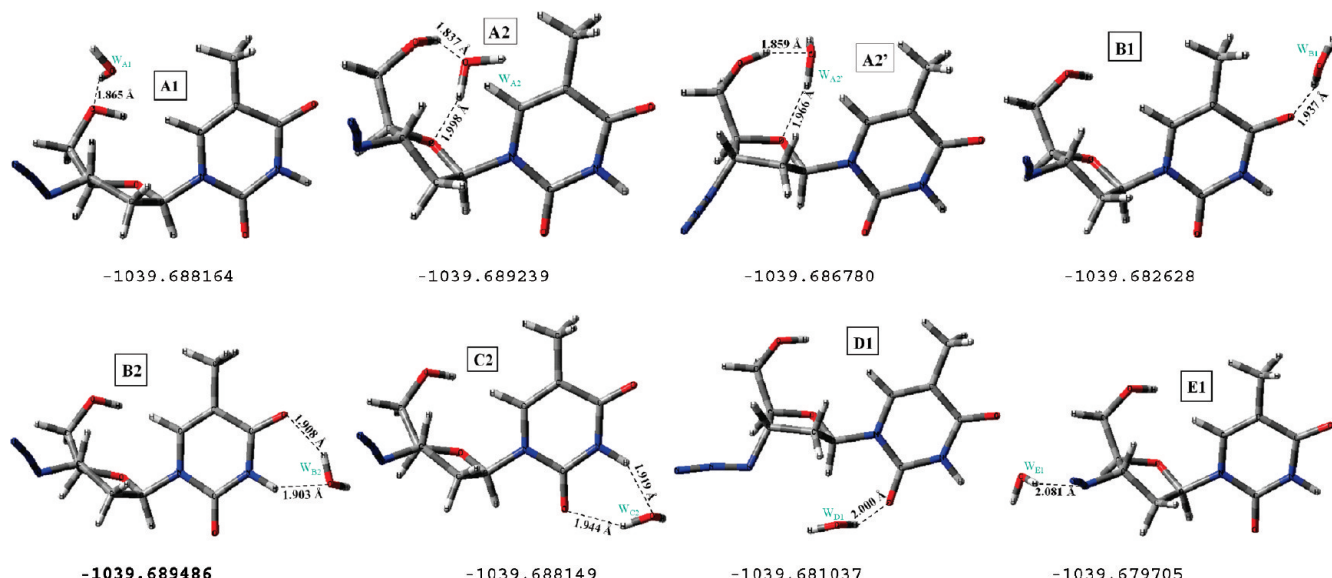


**Figure 3.** Optimum positions of the water molecule in the monohydration of conformer I in AZT. The calculated intermolecular H-bonds and the total energy + ZPE correspond to the B3LYP/6-31G\*\* level.

labeled as A1, A2, A2', B1, B2, C2, D1, E1, E2, and F1, where the number 1 or 2 refers to the number of intermolecular H-bonds of the water molecule. Thus, each water molecule is denoted in reference to its position. H-bond distances are included in each figure, but for simplicity, weak H-bonds are omitted. At the bottom of each structure are listed the total energies of the cluster at the B3LYP level (with ZPE correction) and MP2 level (values in parentheses). The cluster with minimum energy is shown in bold type. In the furanose moiety appear only three places for H-bonds to water molecules, namely, the O5'-H5' group, the O4' atom, and N3' atom, although in the last case, the binding is too weak and the cluster is less stable.

All of the structures are characterized by a planar thymine ring. The monohydration of conformer II differs from that of conformer I: the A1, A2, and A2' clusters are not stable in conformer II (the barrier height corresponding to the  $\beta$  torsional angle is low), and by contrast, the F1 cluster is not stable in conformer I. The two H-bonds of the water molecule in A2 force the  $\beta$  angle to the value of 89.6° (Table 3; 68.8° in the isolated state), impeding the stability of conformer II with a  $\beta$  value of 176.5°.

The relative stability order of conformer I (Figure 3) is

$$\begin{array}{ccccccccccc} \text{B2} & > & \text{A2} & > & \text{A1} & > & \text{C2} & > & \text{A2}' & > & \text{B1} & > & \text{D1} & > & \text{E1} \\ 0 & & 0.15 & & 0.83 & & 0.84 & & 1.70 & & 4.30 & & 5.30 & & 6.14 \end{array} \text{ (kcal·mol}^{-1} \text{ at the B3LYP level)}$$

whereas that for conformer II (Figure 2) is

$$\begin{array}{ccccccccccc} \text{B2} & > & \text{C2} & > & \text{D1} & > & \text{F1} & > & \text{E2} & > & \text{B1} & > & \text{E1} \\ 0 & & 0.76 & & 3.18 & & 2.97 & & 5.46 & & 4.06 & & 5.26 \end{array} \text{ (kcal·mol}^{-1} \text{ at the B3LYP level})$$

$$\begin{array}{ccccccccccc} 0 & & 0.50 & & 2.28 & & 2.95 & & 3.87 & & 4.07 & & 4.18 \end{array} \text{ (kcal·mol}^{-1} \text{ at the MP2 level})$$

These relative energies are consistent with those calculated in the D4T–water system.<sup>14a</sup> The most stable cluster corresponds to B2 at both the B3LYP and MP2 levels, in accordance with the results found for the uracil molecule.<sup>23e</sup> These results indicate that the B3LYP method reproduces well the MP2 pattern of stability order, although some significant differences appear.

The water molecule in position B2 represents the maximum CP-corrected complex formation energy ( $E_{\text{AZTW}_1}^{\text{CP}}$ ) and interaction energy between AZT and the water molecule,  $\Delta E_{\text{AZT}-(\text{W}_1)}^{\text{CP}}$  (Figure 1 in the Supporting Information and Table 4), and thus this position is the most stable one. By contrast, the water molecules in positions E1 and E2 are the least stable and, consequently, have the minimum value of the interaction energy. In positions A2' and D1 of conformer I, the AZT structure shows the maximum deformation energy,  $E_{\text{AZT}}^{\text{def}}$ , whereas in conformer II, the maximum value of  $E_{\text{AZT}}^{\text{def}}$  corresponds to F1. The highest deformation of the water molecule,  $E_{\text{W}_1}^{\text{def}}$ , appears in the B2 and C2 clusters of conformer II because the two H-bonds are strong and of similar strength, whereas in conformer I, it is in A1 and A2'.

**TABLE 3:** Optimum Parameters Calculated in the Different Monohydration Forms of AZT Conformers I and II at the B3LYP/6-31G\*\* and MP2/6-31G\* Levels, Torsional Angles (deg), Phase Angle of Pseudorotation  $P$  (deg), Sugar Conformation, and Dipole Moment  $\mu$  (D)

cluster	method	$\chi$	$\beta$	$\gamma$	$P^a$	sugar conformation	$\mu$
Conformer I							
A1	B3LYP	-110.3	51.7	68.0	67.82	$\frac{1}{4}T$	4.34
A2	B3LYP	-135.3	89.6	58.3	41.86	$\frac{3}{4}T$	1.46
A2'	B3LYP	-120.3	87.7	54.2	107.54	$\frac{1}{4}T$	3.49
B1	B3LYP	-130.3	70.2	61.87	56.70	$\frac{1}{4}E$	4.30
B2	B3LYP	-132.1	69.4	62.37	56.06		3.29
C2	B3LYP	-127.37	69.29	61.38	57.73	$\frac{1}{4}E$	4.54
D1	B3LYP	-127.77	71.27	56.84	109.78	$\frac{1}{4}T$	3.99
E1	B3LYP	-131.69	71.04	60.70	56.21	$\frac{1}{4}E$	3.04
Conformer II							
B1	B3LYP	-126.6	176.7	50.0	166.26	$\frac{1}{2}E$	6.27
	MP2	-125.8	176.6	48.9	164.97		7.69
B2	B3LYP	-126.9	176.9	49.8	165.59		7.26
	MP2	-126.3	176.5	48.9	164.40		8.55
C2	B3LYP	-125.7	176.2	49.2	165.98	$\frac{1}{2}E$	7.12
	MP2	-125.7	175.9	48.6	164.60		8.53
D1	B3LYP	-129.1	177.7	50.8	166.56	$\frac{1}{2}E$	6.30
	MP2	-129.4	176.8	50.4	163.49		8.35
E1	B3LYP	-129.2	178.2	50.5	162.88	$\frac{1}{2}E$	5.66
	MP2	-128.0	177.4	50.2	162.58	$\frac{1}{2}E$	7.29
E2	B3LYP	-123.5	177.8	48.5	176.26	$\frac{3}{2}T$	6.70
	MP2	-123.9	177.2	47.8	170.98	$\frac{1}{2}E$	8.23
F1	B3LYP	-126.6	-88.4	52.3	170.51	$\frac{1}{2}E$	9.27
	MP2	-125.9	-88.6	51.6	168.86		10.44

<sup>a</sup>  $\text{tg}P = [(\nu_4 + \nu_1) - (\nu_3 + \nu_0)] / \{2\nu_2[\sin(36) + \sin(72)]\}$ . When  $\nu_2$  is negative, 180° is added<sup>20</sup> to the calculated value of  $P$ .

**TABLE 4:** CP-Corrected Complex Formation Energy  $\Delta E_{\text{AZTW}_1}^{\text{CP}}$ , Interaction Energy  $\Delta E_{\text{AZT-(W}_1)}^{\text{CP}}$ , and Deformation Energy  $\Delta E_{\text{AZTW}_1}^{\text{def}}$  between AZT and the Water Molecule, in kcal/mol, Calculated at the B3LYP/6-31G\*\* and MP2/6-31G\* Levels in All of the Monohydration Clusters with AZT

cluster	conformer I			conformer II			MP2		
	B3LYP			B3LYP			MP2		
	$\Delta E_{\text{AZTW}_1}^{\text{CP}}$	$\Delta E_{\text{AZT-(W}_1)}^{\text{CP}}$	$\Delta E_{\text{AZTW}_1}^{\text{def}}$	$\Delta E_{\text{AZTW}_1}^{\text{CP}}$	$\Delta E_{\text{AZT-(W}_1)}^{\text{CP}}$	$\Delta E_{\text{AZTW}_1}^{\text{def}}$	$\Delta E_{\text{AZTW}_1}^{\text{CP}}$	$\Delta E_{\text{AZT-(W}_1)}^{\text{CP}}$	$\Delta E_{\text{AZTW}_1}^{\text{def}}$
A1	-12.17	-12.36	1.31	—	—	—	—	—	—
A2	-13.17	-13.24	0.76	—	—	—	—	—	—
A2'	-11.33	-11.51	2.49	—	—	—	—	—	—
B1	-8.42	-8.47	0.20	-8.74	-8.78	0.17	-8.51	-8.92	0.18
B2	-13.09	-13.22	0.49	-13.10	-13.24	0.46	-12.58	-12.68	0.37
C2	-12.19	-12.29	0.48	-12.29	-12.39	0.42	-12.08	-12.16	0.36
D1	-7.00	-7.04	2.48	-9.46	-9.50	0.23	-10.30	-10.34	0.34
E1	-6.27	-6.27	0.11	-7.14	-7.17	0.03	-8.40	-8.44	0.07
E2	—	—	—	-7.37	-7.38	0.05	-8.71	-8.74	0.03
F1	—	—	—	-9.58	-9.62	1.44	-9.63	-9.65	1.74

**Effects of Monohydration.** The main effects of monohydration are the following: (i) A small lengthening by 0.01–0.02 Å is observed in the N–H and C=O bonds involved in the intermolecular H-bonds. As expected, the C–H bonds are not sensitive to the presence of water, and the C<sub>methyl</sub>–H bond has a very small lengthening.

(ii) The negative charges on the oxygen and amino nitrogen atoms are markedly enhanced, and the positive charge of the hydrogens involved in H-bonds is increased. The value of the charge on the N3'' azide nitrogen is close to that on the neighboring C–H hydrogen atoms. Thus, the water molecules are not H-bonded, or are only weakly H-bonded.

(iii) A general increment of the dipole moment  $\mu$  is observed. The F1 cluster has the highest dipole moment.

(iv) An increase occurs in the pseudorotation phase angle  $P$ . The D2 cluster brings about the greatest change in the furanose ring conformation for both conformers I and II.

**3.2.2. AZT–(H<sub>2</sub>O)<sub>n</sub>, n = 2–13.** Following the same methodology,<sup>14</sup> a second water molecule was added to the most stable

monohydrated cluster, B2. Five possible cluster combinations were optimized in conformer I (Figure 4), labeled as B2–B1, B2–C2, B2–D1, B2–E2, and B2–F1. Each letter of this notation corresponds to one water molecule. To confirm that we actually obtained the most stable cluster with two water molecules, other combinations were also optimized. These combinations were always less stable than those obtained with the water molecule in B2 and thus they were not included in Figure 4. Because of the high computational demand, calculations at the MP2 level were not possible. For simplicity, the results for conformer I are not included.

Following the same methodology as before, the 3rd through 13th water molecules were added sequentially (Figure 5). For clarity, in the notation used for the clusters, only the last two water molecules appear. In general, each water molecule is denoted in reference to its position, but when they cannot be clearly identified, as for W<sub>5</sub> to W<sub>13</sub>, they are denoted in reference to the number of water molecule added. B3LYP reproduces well the stability trend in the hydration of AZT, as compared to that

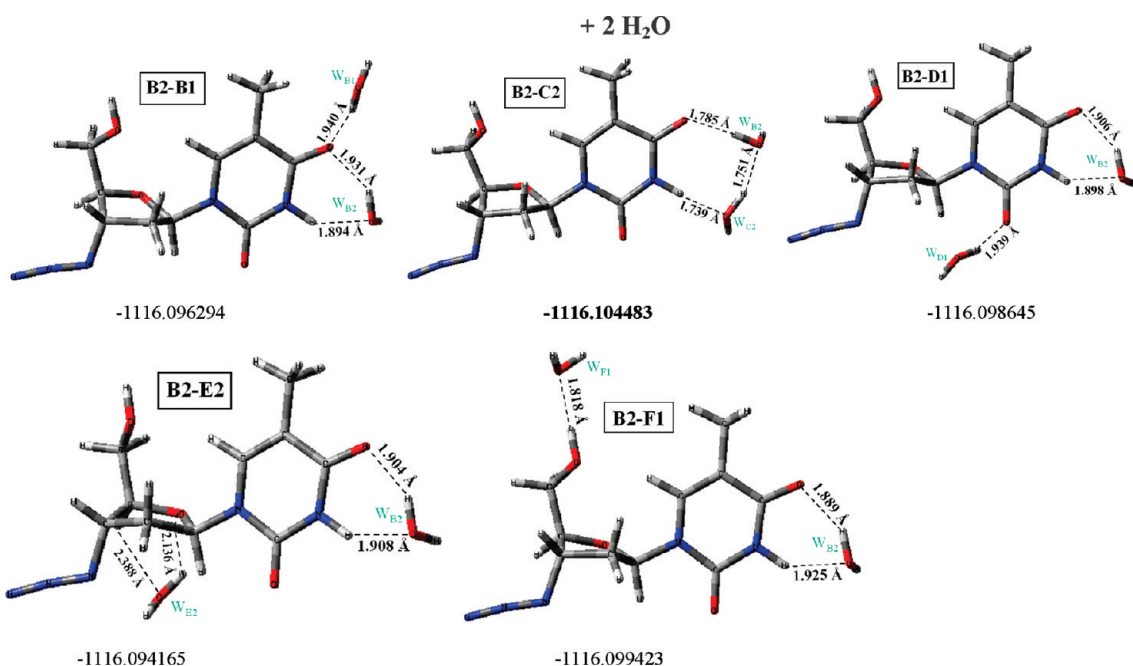


**Figure 4.** Optimum positions of two water molecules in the hydration of conformer II in AZT.

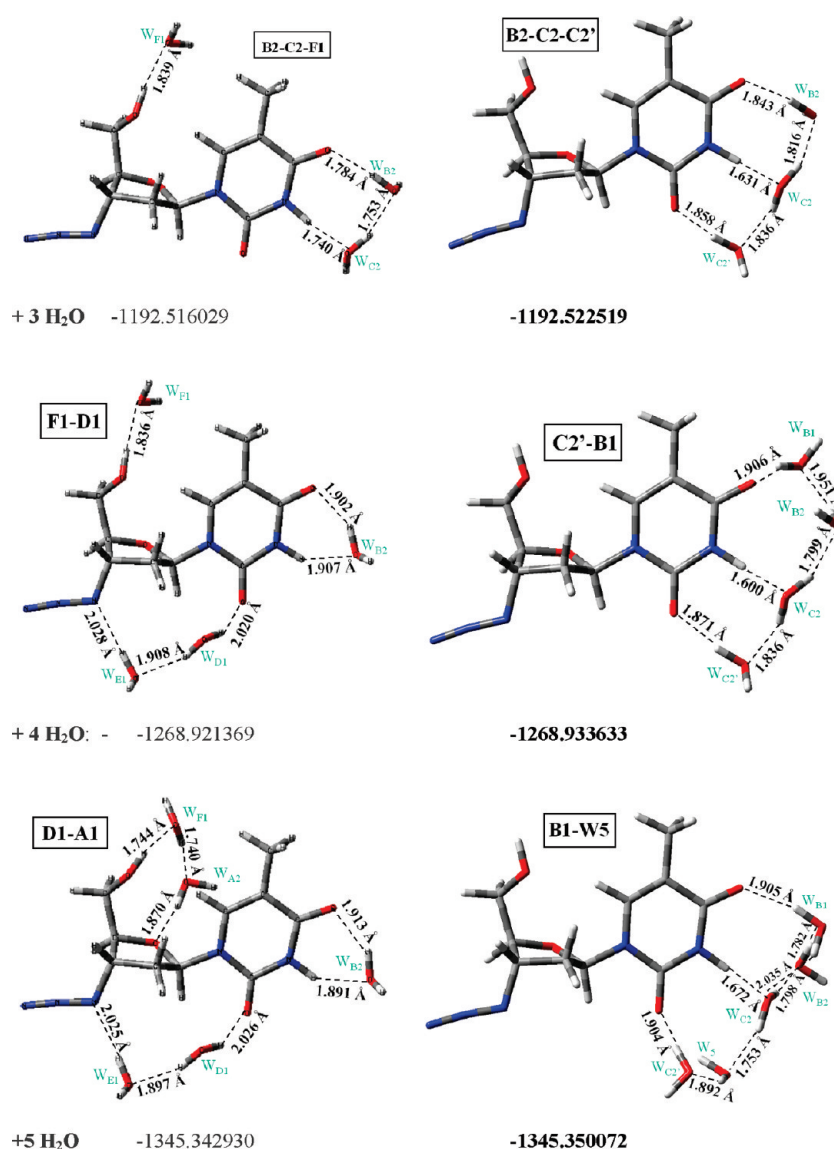


**Figure 5.** Continued.

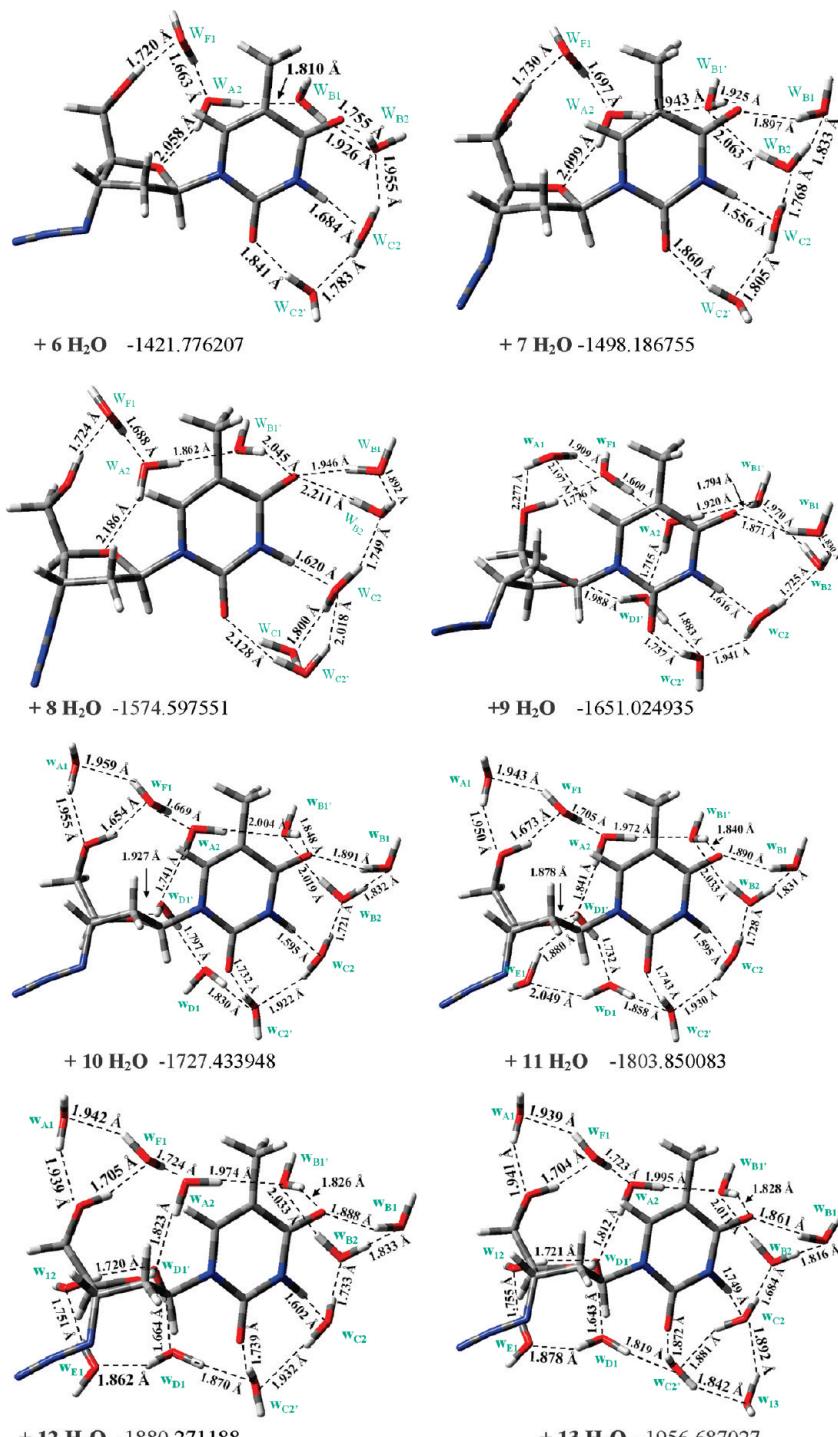


**Figure 5.** Optimum forms for 3 to 13 water molecules in the simulation of the first hydration shell of conformer II-I in AZT. The calculated intermolecular H-bonds and the total energy + ZPE (in au) correspond to the B3LYP/6-31G\*\* level.

obtained in D4T<sup>14</sup> and Thy (Figure 6). Conformer I follows a different trend in the addition of the second through eighth water molecules, and for simplicity, we do not discuss it.

It is noted that, in general, there is a significant change in the  $\chi$  and  $\beta$  torsional angles when the sixth water molecule is introduced (Table 2), as well as the ninth water molecule. In this last case conformer II changes to conformer I, by rotation of the  $\beta$  torsional angle, with a value of 60–70°. Thus, conformer I is the only stable one upon the further addition of water molecules. This is due to the preference for H-bonds among water molecules rather than between water and AZT. This cluster shows the highest deformation energy (Figure 2 of

the Supporting Information) with different pseudorotation phase angles  $P$  and sugar conformations. The further addition of water molecules increases the complexity of the hydration pattern, which is derived from the extraordinary variety of orientations displayed by the water molecules. The resulting orientations of these water molecules are represented by the complicated network of H-bonds, as shown in Figure 5 for 13 water molecules, where  $W_{A2}$  and  $W_{D1'}$  are the central water molecules. We expect that adding second-shell water molecules to the system would not qualitatively change the results.

In our calculations, the first hydration shell is approximately completed with 13 water molecules, in accordance with the

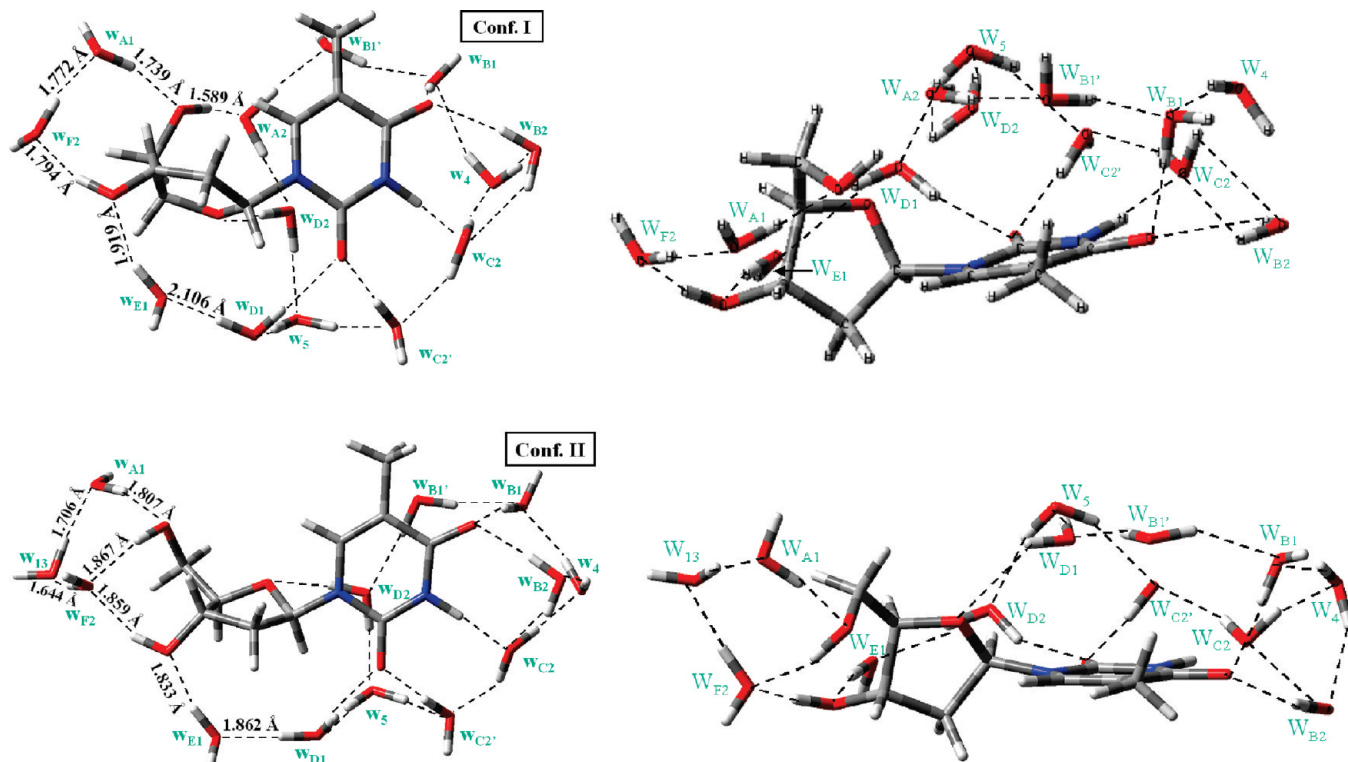


**Figure 6.** Two views of the two most optimum clusters (conformers I and II) of thymidine with 13 water molecules.

estimated experimental number of hydration water molecules,<sup>44,45</sup> between 6 and 10 per nucleotide. Moreover, the hydration of guanine<sup>46</sup> in the first solvation shell included 7–13 water molecules. Other experimental studies on methyl-substituted uracils and thymines indicated that, when more than four water molecules are attached, the photophysical properties of these hydrated clusters should rapidly approach those in the condensed phase.<sup>47</sup>

*First Hydration Shell Effects and Characteristics.* The effects and characteristics of the first hydration shell can be summarized as follows:

(i) Hydration reduces the number of conformers calculated in the isolated state. The clusters obtained in the hydration of conformers I and II show a higher stability than those obtained in the hydration of other conformers. We found another cluster with 13 water molecules to be more stable than that of Figure 5, but the  $\chi$  value of  $-66^\circ$  appears out of the range for anti form for expected biological activity, so it was not included in the present article.

(ii) Some regular orientation of the water molecules in the first hydration shell occurs: the direction of hydration is marked for the first water molecule, and it can be observed with the successive additions. All of the water molecules appear to be H-bonded at the same face of the AZT molecule, because (a) the H-bonds between water molecules are more stable than those between a water molecule and the nucleoside and (b) a small water network appears upon addition of the sixth water molecule.

(iii) Some similarities with the hydration of Thy are observed in regions B and C (Figure 6). The optimum distribution of the water molecules, binding to the most polar groups, is in general in accordance with the previous hydrated structure found in D4T.<sup>14</sup>

In the isolated state, conformer II, with a higher dipole moment (7.79 D by MP2) than conformer I (3.76 D), is favored in a polarizable environment with successive hydration, although,

because of the strong H-bond net, with more than nine water molecules, only conformer I prevail.

(iv) Water molecules are not H-bonded (or are bonded with a weak stretch) to the azide group, because of the low reactivity of this group. Thus, the hydration of the furanose moiety differs from that of Thy. Moreover, conformers I and II are stable in the cluster of Thy with 13 water molecules, because of the fact that, in Thy, a water dimer can be H-bonded to O3'-H and O5'-H, thereby stabilizing conformer II.

(v) The water molecules affect the planarity of the pyrimidine ring only slightly, with changes in its torsional angles of less than  $2^\circ$ . However, a lengthening of the C=O, N-H, and O-H bonds and an opening of the N-C-N and N3-C-C ring angles involved in H-bonds are observed. The methyl group remains little affected by the water molecules. The optimized values with  $\chi$  in trans and  $\gamma$  (ca.  $60^\circ$ ) agree well with those reported from NMR studies in solution.<sup>38b</sup>

The calculated O<sub>w</sub>—H<sub>w</sub> bonds of the water molecules are significantly longer than those in the isolated state and in the bulk (PCM calculations) because of the strong H-bond interactions.

(vi) The degree of pucker,  $\nu_{\max}$ , which is sensitive to inter- and intramolecular interactions, increases with hydration, and it is markedly higher than in Thy (Table 5) because of the different hydration pattern. As a consequence, the flexibility of hydrated AZT is higher than that of hydrated Thy.

(vii) Hydration reduces or breaks all of the weak intramolecular H-bonds observed in the isolated state of AZT. Because of the rotation of the thymine and furanose rings through the effects of the 13 water molecules, the O4'…H6 and O5'…H6 H-bonds disappear and O2…H1' remains weak.

(viii) A general enhancement of the charges is observed, especially the negative charges on the oxygen atoms and the positive charge on N3-H (Figure 1), because of the strong H-bonds with water and the polarizing effect of water on the solute charge distribution. These features increase the reactivity

**TABLE 5: Geometrical Features: Torsional Angles (deg), in Conformers I and II (in Parentheses) of AZT and Thy, Optimized at the B3LYP/6-31G\*\* and MP2/6-31G\*\* Levels**

parameters	AZT (isolated state)	AZT (isolated state)	MP2	AZT (crystal <sup>c</sup> )	AZT + 3H <sub>2</sub> O	AZT (PCM)	AZT +13H <sub>2</sub> O	Thy +13H <sub>2</sub> O
Exocyclic Torsion Angles								
$\gamma$ (O5'-C5'-C4'-C3' or O5'-C5'-C4'-O4')	61.9 (50.2)	61.9 (49.2)		50.9 (49.9)		59.7 (50.1)	52.2	51.2 (35.8)
	-55.0 (-69.4)	-54.4 (-69.6)		-67.9 (-69.7)		-58.2 (-69.3)	-64.7	-69.4 (-82.8)
$\chi$ (O4'-C1'-N1-C2 or O4'-C1'-N1-C6)	-129.1 (-128.1)	-133.4 (-126.9)		-124.4 (-127.0)		-143.1 (-125.8)	-101.9	-88.4 (-131.6)
$\delta$ (C5'-C4'-C3'-O3' or C5'-C4'-C3'-N')	50.4 (49.6)	48.9 (50.3)		(49.9)	39.9 (51.7)	63.8	75.8 (35.3)	
$\epsilon$ (C2'-C3'-N3'-N3'' or C2'-C3'-O3'-H3')	87.3 (140.0)	85.1 (144.6)		(144.9)	85.0 (144.6)	138.8	116.9 (85.5)	
$\nu_0$ (C4'-O4'-C1'-C2')	95.9 (70.9)	85.0 (63.8)		177.5	173.3	102.4 (77.0)	179.6	160.5 (165.3)
Endocyclic Torsion Angles								
$\nu_1$ (O4'-C1'-C2'-C3')	-7.6 (-19.4)	-5.3 (-21.5)		(-18.4)	-3.3 (-14.7)	-33.1	-0.9 (-39.5)	
$\nu_2$ (C1'-C2'-C3'-C4')	-14.0 (31.6)	-17.7 (34.7)		(31.6)	-18.8 (29.7)	39.7	-0.4 (18.2)	
$\nu_3$ (C2'-C3'-C4'-O4')	28.3 (-31.1)	32.3 (-34.1)		(-31.8)	31.9 (-32.6)	-31.6	1.5 (7.8)	
$\nu_4$ (C3'-C4'-O4'-C1')	-33.3 (20.6)	-36.1 (22.5)		(22.0)	-34.5 (24.8)	13.3	-2.1 (-31.4)	
$P^a$	26.2 (-0.9)	26.4 (-0.79)		(-2.3)	24.2 (-6.5)	12.3	1.9 (44.4)	
$\nu_{\max}^b$	31.32 (162.89)	26.80 (162.65)		(144.89)	23.71 (172.52)	116.80	44.27 (79.81)	
	33.15 (32.53)	36.14 (35.76)		(38.92)	34.87 (32.84)	70.18	2.09 (44.07)	

<sup>a</sup> tgP = [( $\nu_4 + \nu_1$ ) - ( $\nu_3 + \nu_0$ )]/{2 $\nu_2$ [sin(36) + sin(72)]}. <sup>b</sup>  $\nu_{\max}$  =  $\nu_2/(\cos P)$  <sup>c</sup> In AZTA, ref 28a.

of AZT and are accompanied by an increase in the energies of the highest occupied and lowest unoccupied molecular orbitals.

**Deformation Energies.** Figures 2–4 of the Supporting Information show plots of the calculated deformation energies for AZT and water molecules as a consequence of the successive addition of water molecules. The deformation energies of each water molecule in the complex are plotted in Figure 4 of the Supporting Information. W<sub>F1</sub> and W<sub>C2'</sub> are the water molecules that remain more strongly H-bonded to AZT, whereas W<sub>C2</sub> and W<sub>C2'</sub> are those most H-bonded to other water molecules and to AZT. The three atoms of W<sub>C2</sub> participate in strong H-bonds, with one of them, H<sub>W<sub>C2</sub></sub>...O<sub>W<sub>B2</sub></sub>, having the short distance of 1.684 Å in the AZT-(H<sub>2</sub>O)<sub>13</sub> cluster (Figure 5). Also, W<sub>D1</sub> appears with a strong H-bond with a length of 1.643 Å. As consequence of this short H-bond, W<sub>D1</sub> and W<sub>C2'</sub> suffer the highest deformation and have a jump in deformation energy to values of ca. 0.6 kcal/mol. This jump appears with the addition of the fifth to seventh water molecules, and it increases slightly upon further hydration. W<sub>D1'</sub>, W<sub>F1</sub>, and W<sub>B2</sub> also increase the deformation with the addition of the sixth and seventh water molecules. This is due to the new molecules W<sub>A2</sub> and W<sub>F1</sub> connecting region A with regions B and C, slightly compressing the structure and reducing the O5'...O2 and O4...O4' distances.

Because of the high deformation observed in W<sub>C2'</sub>, this molecule and its neighbors W<sub>B2</sub> and W<sub>C2</sub> were studied in Figure 2 of the Supporting Information. The deformation energies of these molecules (now labeled as W<sub>2</sub>, W<sub>1</sub>, and W<sub>3</sub>, respectively) are shown in comparison with that calculated in AZT. It can be noted that the deformation energy is much higher in AZT than in the water molecules. In conformer II, the deformation energy increases with increasing hydration until the high value of 6 kcal/mol is reached with eight water molecules. A further addition of water molecules produces a change to conformer I and a stabilization of the energy value.

Figure 3 of the Supporting Information shows the calculated complex formation and interaction energies for AZT–water and water–water. The CP-corrected interaction energy for AZT–water,  $\Delta E_{AZT-(W_n)}^{CP}$ , has larger values than that corresponding to the AZT molecule and water–water, and the difference increases with the hydration. This behavior differs with that found in

**TABLE 6: Intramolecular Distances of Interest among the Reactive Oxygen Atoms Calculated in Conformers I and II (in Parentheses) of AZT**

distance	B3LYP	MP2	B3LYP	B3LYP
	isolated state	isolated state	PCM	+ 13H <sub>2</sub> O
O5'...O2	6.262 (6.123)	6.221 (6.082)	6.362 (6.045)	6.267
O5'...O4	6.807 (6.901)	6.678 (6.860)	6.784 (6.723)	7.322
O5'...O4'	2.787 (2.909)	2.759 (2.885)	2.869 (2.938)	2.901

D4T,<sup>14</sup> where  $\Delta E_{D4T-W_n}^{CP}$  is always higher than  $\Delta E_{W_n}^{CP}$  and  $\Delta E_{D4T-(W_n)}^{CP}$ . Moreover, because of the structure of D4T, the AZT–water interactions are more than 2 times higher than D4T–water interactions, and with the progress of hydration, the water molecules appear to be more strongly H-bonded among themselves and more weakly H-bonded with D4T.

**Intramolecular Distances.** Distances between the most reactive atoms, such as the oxygens, for isolated and hydrated forms in the conformers under study are collected in Table 6. The interest in these values is their relation with the possible binding sites in the kinase,<sup>48</sup> which will be the next step in our work.

In the isolated state, the puckering of the furanose ring is slightly smaller in AZT than in Thy, and it brings O4' and O5' nearer, 2.76 Å by MP2 compared to 2.78 Å in Thy, as well as decreasing the O5'...O2 and O5'...O4 distances, to 6.221 and 6.678 Å, respectively, compared to 6.273 and 7.255 Å in Thy.

By contrast, in the hydration with 13 water molecules, the H-bonded water net with Thy is slightly stronger than that with AZT. This fact, together with the smaller furanose ring pucker in Thy, produces a closeness of the O5'-H moiety to the O4 atom through W<sub>A2</sub> and W<sub>D2</sub> and leads to markedly lower O5'...O2, O5'...O4, and O5'...O4' length values (5.701, 6.178, and 2.956 Å, respectively) than in AZT. In conformer II of Thy, water molecules W<sub>F2</sub> and W<sub>13</sub> (Figure 6) produce an opening of the structure and the longest O5'...O2 and O5'...O4 distances.

**3.2.3. PCM.** With the PCM, the number of stable conformers<sup>15</sup> was markedly reduced (Table 1). Thus, conformer I appears as a saddle point, whereas conformer II corresponds to a stable minimum. This fact has also been observed for conformers I and II of Thy and D4T.<sup>14</sup> However, with nine explicit water

molecules, conformer II is not stable, and it changes to conformer I. This is because, in the PCM, the external polar cavity attracts the hydrogen of the O5'-H group to a more open structure such as conformer II. However, this model fails when water molecules can be introduced in the holes inside the molecule, such as W<sub>A2</sub> in the D4T, Thy, and AZT molecules, where closer structures are favored, such as conformer I. Thus, we can conclude that conformer I in AZT is one of the main forms present in the first hydration shell.

The effect of hydration on the geometry of AZT is smaller with the PCM than with discrete methods. For the atomic charges, the values are close to those of the isolated state, whereas with the DM, the differences are significant (Figure 1). The PCM does not reproduce well the hydration pattern of AZT.

Table 5 shows the changes observed for Thy and AZT, in the isolated state and under hydration. The pseudorotation phase angle  $P$ , the torsional angles of the furanose ring, and the maximum torsion angle  $\nu_{\max}$  are also included. With PCM, a marked variation in these angles is observed in the two conformers of AZT. With 13 explicit water molecules, conformer I in Thy shows very little endocyclic torsional angles that render the furanose ring nearly planar, but the same does not occur in AZT. The values of  $P$  and  $\nu_{\max}$  are markedly lower in Thy than in AZT.

A database of hydrated DNA X-ray structures shows that the water molecule can be found either in region A or in regions C and D. Because of their high mobility caused by the presence of large hydrophobic methyl groups, water molecules in region A were observed only in high-resolution, low-temperature B-DNA structures, whereas hydration in regions C and D is much more localized.<sup>44,49</sup> In B-DNA crystals, water molecules are also found in a position between region D and the methyl group.<sup>44</sup> In these structures, the water is weakly H-bonded to the C-H of the methyl group (interaction found in our calculations) and stabilized by the interaction with the phosphate group.

#### 4. Summary and Conclusions

HIV constitutes a serious worldwide problem and continues to pose a major challenge to the international multidisciplinary scientific community. Any information that could shed light on this problem is important. We focused in this work on AZT and Thy, for the effects of the hydration on structural parameters, interatomic distances, H-bonds, dipole moments, and NBO charges of selected atoms and the influence of water on the stability of the different conformers. The geometries and values of the properties presented here appear to be the most accurate to date. Good agreement was obtained, whenever available, with analogous theoretical studies. More than 200 cluster-optimized structures with water molecules were determined for the first time at the MP2 and B3LYP levels. Very slight differences in the conformational angles appear between the MP2 and B3LYP results. Hydration reduces the population of conformers determined in the isolated state. With few water molecules, the AZT structure is markedly deformed, but the deformation remains stable with more than nine water molecules. We determined the most stable AZT-13H<sub>2</sub>O cluster. The values of  $\chi$  and  $\gamma$  angles in this cluster agree well with those reported based on NMR studies in solution. Hydration produces a marked reduction of the intramolecular H-bonds between the sugar and the base. The PCM markedly underestimates the deformation of the structure by the water molecules. Our results indicate that AZT exhibits conformational profiles similar to those of its

parent natural nucleoside Thy. Because of this similarity, AZT mimics Thy in biological systems and becomes incorporated into viral DNA, thereby bringing about the termination of DNA synthesis. A good comprehension of the parameters investigated could be essential for developing drugs with high anti-HIV activity.

**Acknowledgment.** The authors thank the UCM of Spain for financial support through UCM-BSCH GR58/08 Grant 921628 and the MCI through CTQ2010-18564 (subprogram BQU).

**Supporting Information Available:** Formation and interaction energies under hydration (Figures 1-4). This information is available free of charge via the Internet at <http://pubs.acs.org>.

#### References and Notes

- (a) Weiss, R. A. *Science* **1993**, *260*, 1273. (b) Kuipers, M. E.; Swart, P. J.; Hendriks, M. M. W. B.; Meijer, D. K. F. *J. Med. Chem.* **1995**, *38* (6), 883.
- (2) Ciuffo, G. M.; Santillan, M. B.; Estrada, M. R.; Yamin, L. J.; Jáuregui, E. A. *J. Mol. Struct. (THEOCHEM)* **1998**, *428*, 155.
- (3) (a) De Clercq, E. *Int. J. Antimicrob. Agents* **2009**, *33* (4), 307. (b) Khandazhinskaya, A. L.; Yanvarev, D. V.; Jasko, M. V.; Shipitsin, A. V.; Khalizev, V. A.; Shram, S. I.; Skoblov, Y. S.; Shirokova, E. A.; Kukhanova, M. K. *Drug Metab. Dispos.* **2009**, *37* (3), 494. (c) Urso, P.; Goldberg, B.; De Lancie, R.; Margulis, S. B. *Life Sci. J.* **2008**, *5* (3), 41.
- (4) (a) Taft, C. A.; Paula da Silva, C. H. T. *Curr. Comput.-Aided Drug Des.* **2006**, *2* (3), 307. (b) Tandon, V. K.; Chhor, R. B. *Curr. Med. Chem.: Anti-Infect. Agents* **2005**, *4* (1), 3.
- (5) Raviolo, M. A.; Breva, I. C.; Esteve-Romero, J. *J. Chromatogr. A* **2009**, *1216* (16), 3546.
- (6) (a) Al-Masoudi, N. A.; Essa, A. H. *J. Comput. Theor. Nanosci.* **2008**, *5* (11), 2216. (b) Donnerer, J.; Haas, B. J.; Kessler, H. H. *Pharmacology* **2008**, *82* (4), 287. (c) Vela, J. E.; Miller, M. D.; Rhodes, G. R.; Ray, A. S. *Antiviral Ther.* **2008**, *13* (6), 789.
- (7) Arissawa, M.; Taft, C. A.; Felcman, J. *Int. J. Quantum Chem.* **2003**, *93*, 422.
- (8) (a) De Clercq, E. *J. Clin. Virol.* **2001**, *22* (1), 73. (b) Kayitare, E.; Vervaet, C.; Ntawukulilyayo, J. D.; Seminega, B.; Bortel, V.; Remon, J. P. *Int. J. Pharm.* **2009**, *370* (1-2), 41. (c) De Clercq, E. *Biochim. Biophys. Acta* **2002**, *1587* (2-3), 258. (d) Newman, D. J.; Cragg, G. M.; Snader, K. M. *Nat. Prod. Rep.* **2000**, *17* (3), 215. (e) Vortherms, A. R.; Dang, H. N.; Doyle, R. P. *Clin. Med.: Oncol.* **2009**, *3*, 19.
- (9) U.S. Food and Drug Administration (FDA). <http://www.fda.gov>.
- (10) (a) Naeger, L. K.; Margot, N. A.; Miller, M. D. *Antimicrob. Agents Chemother.* **2002**, *46* (7), 2179. (b) Pornprasert, S.; Mary, J.-Y.; Faye, A.; Leechanachai, P.; Limtrakul, A.; Rugpao, S.; Sirivatanapa, P.; Gomuthbutra, V.; Matanasaravoot, W.; Le Coeur, S.; Lallement, M.; Barré-Sinoussi, F.; Menu, E.; Ngo-Giang-Huong, N. *Curr. HIV Res.* **2009**, *7* (2), 211. (c) Violari, A.; Cotton, M. F.; Gibb, D. M.; Babiker, A. G.; Steyn, J.; Madhi, S. A.; Jean-Philippe, P.; McIntyre, J. A. N. *Engl. J. Med.* **2008**, *359* (21), 2233. (d) Seaton, R. A.; Fox, R.; Bodasing, N.; Peters, S. E.; Gourlay, Y. *Aids* **2003**, *17* (3), 445.
- (11) (a) Tortorella, C.; Guidolin, D.; Petrelli, L.; De Toni, R.; Milanesi, O.; Ruga, E.; Rebuffat, P.; Bova, S. *Int. J. Mol. Med.* **2009**, *23* (6), 799. (b) Kline, E. R.; Bassit, L.; Hernandez-Santiago, B. I.; Detorio, M. A.; Liang, B.; Kleinhenz, D. J.; Walp, E. R.; Dikalov, S.; Jones, D. P.; Schinazi, R. F.; Sutliff, R. L. *Cardiovasc. Toxicol.* **2009**, *9* (1), 1.
- (12) Yekeler, H. *J. Mol. Struct. (THEOCHEM)* **2004**, *684*, 223.
- (13) Van Roey, P.; Taylor, E. W.; Chu, C. K.; Schinazi, R. F. *J. Am. Chem. Soc.* **1993**, *115*, 5365.
- (14) (a) Alcolea Palafox, M.; Iza, N.; de la Fuente, M.; Navarro, R. *J. Phys. Chem. B* **2009**, *113* (8), 2458. (b) Alcolea Palafox, M.; Niza, N. *Phys. Chem. Chem. Phys.* **2010**, *12* (4), 881.
- (15) Alcolea Palafox, M.; Talaya, J. *J. Phys. Chem. B*, manuscript in preparation.
- (16) (a) Borojerdi, J. P.; Ming, J.; Cooch, C.; Ward, Y.; Semino-Mora, C.; Yu, M.; Braun, H. M.; Taylor, B. J.; Poirier, M. C.; Olivero, O. A. *Mutat. Res., Fundam. Mol. Mech. Mutagen.* **2009**, *665* (1-2), 67. (b) Desai, V. G.; Lee, T.; Moland, C. L.; Brantham, W. S.; Von Tuneln, L. S.; Beland, F. A.; Fuscoe, J. C. *Mitochondrion* **2009**, *9* (1), 9. (c) Duy, S. V.; Lefebvre-Tournier, I.; Pichon, V.; Hugon-Chapuis, F.; Puy, J.-Y.; Périgaud, C. *J. Chromatogr. B: Anal. Technol. Biomed. Life Sci.* **2009**, *877* (11-12), 1101. (d) Wang, X.; Chai, H.; Lin, P. H.; Yao, Q.; Chen, C. *Am. J. Pathol.* **2009**, *174* (3), 771. (e) Lynx, M. D.; LaClair, D. D.; McKee, E. E. *Antimicrob. Agents Chemother.* **2009**, *53* (3), 1252. (f) Fang, J.-L.; McGarry, L. J.; Beland, F. A. *Mutagenesis* **2009**, *24* (2), 133. (g) von Kleist, M.; Huisings, W. *Eur. J. Pharm. Sci.* **2009**, *36* (4-5), 532. (h)

- Matteucci, C.; Minutolo, A.; Balestrieri, E.; Ascolani, A.; Grelli, S.; Macchi, B.; Mastino, A. *Pharmacol. Res.* **2009**, 59 (2), 125. (i) Hurwitz, S. J.; Asif, G.; Kivel, N. M.; Schinazi, R. F. *Antimicrob. Agents Chemother.* **2008**, 52 (12), 4241.
- (17) (a) Saran, A.; Ojha, R. P. *J. Biosci.* **1991**, 16 (1–2), 29. (b) Novak, I.; Kovac, B. *J. Org. Chem.* **2003**, 68 (14), 5777. (c) Nava-Salgado, V. O.; Martínez, R.; Arroyo, M. F. R.; Galicia, G. R. *J. Mol. Struct. (THEOCHEM)* **2000**, 504, 69. (d) Monajjem, M.; Abedi, A.; Passdar, H. *Bull. Chem. Soc. Ethiop.* **2006**, 20 (1), 133. (e) Estévez, C. M.; Graña, A. M.; Ríos, M. A. *J. Mol. Struct. (THEOCHEM)* **1993**, 288, 207. (f) Saran, A.; Ojha, R. P. *J. Mol. Struct. (THEOCHEM)* **1993**, 284, 223. (g) Essa, A. H. *J. Comput. Theor. Nanosci.* **2009**, 6 (5), 1059. (h) Arissawa, M.; Felcman, J.; Herrera, J. O. M. *J. Biochem. Mol. Biol.* **2003**, 36 (3), 243. (i) Essa, A. H.; Ibrahim, M.; Hameed, A. J.; Al-Masoudi, N. A. *Arkivoc* **2008**, xiii, 255.
- (18) Xinjuan, H.; Mingbao, H.; Dayu, Y. *Sci. China, Ser. B* **2002**, 45 (5), 470.
- (19) Hernández, J.; Soscún, H.; Hinchliffe, A. *Internet Electron. J. Mol. Des.* **2003**, 2, 589.
- (20) Baumgartner, M. T.; Motura, M. I.; Contreras, R. H.; Pierini, A. B.; Brinón, M. C. *Nucleosides Nucleic Acids* **2003**, 22 (1), 45.
- (21) Frisch, M. J.; Trucks, G. W.; Schlegel, H. B.; Scuseria, G. E.; Robb, M. A.; Cheeseman, J. R.; Montgomery, J. A., Jr.; Vreven, T.; Kudin, K. N.; Burant, J. C.; Millam, J. M.; Iyengar, S. S.; Tomasi, J.; Barone, V.; Mennucci, B.; Cossi, M.; Scalmani, G.; Rega, N.; Petersson, G. A.; Nakatsuji, H.; Hada, M.; Toyota, K.; Fukuda, R.; Hasegawa, J.; Ishida, M.; Nakajima, T.; Honda, Y.; Kitao, O.; Nakai, H.; Klene, M.; Li, X.; Knox, J. E.; Hratchian, H. P.; Cross, J. B.; Adamo, C.; Jaramillo, J.; Gomperts, R.; Stratmann, R. E.; Yazyev, O.; Austin, A. J.; Cammi, R.; Pomelli, C.; Ochterski, J. W.; Ayala, P. Y.; Morokuma, K.; Voth, G. A.; Salvador, P.; Dannenberg, J. J.; Zakrzewski, V. G.; Dapprich, S.; Daniels, A. D.; Strain, M. C.; Farkas, O.; Malick, D. K.; Rabuck, A. D.; Raghavachari, K.; Foresman, J. B.; Ortiz, J. V.; Cui, Q.; Baboul, A. G.; Clifford, S.; Cioslowski, J.; Stefanov, B. B.; Liu, G.; Liashenko, A.; Piskorz, P.; Komaromi, I.; Martin, R. L.; Fox, D. J.; Keith, T.; Al-Laham, M. A.; Peng, C. Y.; Nanayakkara, A.; Challacombe, M.; Gill, P. M. W.; Johnson, B.; Chen, W.; Wong, M. W.; Gonzalez, C.; Pople, J. A. *Gaussian 03*, revision B.04; Gaussian, Inc.: Pittsburgh, PA, 2003.
- (22) (a) Hoffmann, M.; Rychlewski, J. *Rev. Mod. Quantum Chem.* **2002**, 2, 1767. (b) Yurenko, Y. P.; Zhurakivsky, R. O.; Ghomi, M.; Samijlenko, S. P.; Hovorun, D. M. *J. Phys. Chem. B* **2007**, 111, 6263. (c) Yurenko, Y. P.; Zhurakivsky, R. O.; Ghomi, M.; Samijlenko, S. P.; Hovorun, D. M. *J. Phys. Chem. B* **2008**, 112, 1240. (d) Gaigeot, M.-P.; Ghomi, M. *J. Phys. Chem. B* **2001**, 105 (21), 5007. (e) Shishkin, O. V.; Gorb, L.; Leszczynski, J. *Int. J. Mol. Sci.* **2000**, 1, 17.
- (23) (a) Alcolea Palafox, M.; Nielsen, O. F.; Lang, K.; Garg, P.; Rastogi, V. K. *Asian Chem. Lett.* **2004**, 8, 81. (b) Alcolea Palafox, M.; Rastogi, V. K. *Spectrochim. Acta* **2002**, 58 A, 411. (c) Alcolea Palafox, M. *Recent Research Developments in Physical Chemistry*; Transworld Research Network: Kerala, India, 1998; Vol. 2; p 213. (d) Alcolea Palafox, M. *Int. J. Quantum Chem.* **2000**, 77, 661. (e) Alcolea Palafox, M.; Iza, N.; Gil, M. *J. Mol. Struct. (THEOCHEM)* **2002**, 585, 69.
- (24) Jensen, F. *Introduction to Computational Chemistry*; John Wiley & Sons Ltd.: Chichester, U.K., 2002; p 189.
- (25) (a) Tomasi, J.; Mennucci, B.; Cancès, E. *J. Mol. Struct. (THEOCHEM)* **1999**, 464, 211. (b) Cossi, M.; Scalmani, G.; Rega, N.; Barone, V. *J. Chem. Phys.* **2002**, 117 (1), 43. (c) Cossi, M.; Rega, N.; Scalmani, G.; Barone, V. *J. Comput. Chem.* **2003**, 24, 669.
- (26) Reed, A. E.; Curtiss, L. A.; Weinhold, F. *Chem. Rev.* **1988**, 88 (6), 899.
- (27) Saenger, W. *Principles in Nucleic Acid Structure*; Springer Verlag: New York, 1984.
- (28) (a) Van Roey, P.; Salerno, J. M.; Duax, W. L.; Chu, C. K.; Ahn, M. K.; Schinazi, R. F. *J. Am. Chem. Soc.* **1988**, 110, 2277. (b) Allen, F. H.; Bellard, S.; Brice, M. D.; Cartwright, B. A.; Doubleday, A.; Higgs, H.; Hummelink, T.; Hummelink-Peters, B. G.; Kennard, O.; Motherwell, W. D. S.; Rodgers, J. R.; Watson, D. G. *Acta Crystallogr. B: Struct. Crystallogr. Cryst. Chem.* **1979**, B35, 2331.
- (29) Aamouche, A.; Berthier, G.; Cadioli, B.; Gallinella, E.; Ghomi, M. *J. Mol. Struct. (THEOCHEM)* **1998**, 426, 307.
- (30) Williams, R. W.; Cheh, J. L.; Lowrey, A. H.; Weif, A. F. *J. Phys. Chem.* **1995**, 99, 5299.
- (31) Alemán, C. *Chem. Phys. Lett.* **1999**, 302, 461.
- (32) Tomasi, J.; Persico, M. *Chem. Rev.* **1994**, 94 (7), 2027.
- (33) Danilov, V. I.; Van Mourik, T.; Poltev, V. I. *Chem. Phys. Lett.* **2006**, 429, 255.
- (34) Yurenko, Y. P.; Zhurakivsky, R. O.; Ghomi, M.; Samijlenko, S. P.; Hovorun, D. M. *J. Phys. Chem. B* **2007**, 111, 9655.
- (35) (a) Gurskaya, G. V.; Tsapkina, E. N.; Skaptsova, N. V.; Kraevskii, A. A.; Lindeman, S. V.; Struchkov, Y. T. *Dokl. Akad. Nauk SSSR* **1986**, 291, 854. (b) Parthasarathy, R.; Kim, H. *Biochem. Biophys. Res. Commun.* **1988**, 152 (1), 351. (c) Camerman, A.; Mastropaoletti, D.; Camerman, N. *Proc. Natl. Acad. Sci. U.S.A.* **1987**, 84, 8239.
- (36) Dyer, I.; Low, J. N.; Tollin, P.; Wilson, H. R.; Howie, R. A. *Acta Crystallogr. C* **1988**, 44, 767.
- (37) Birnbaum, G. I.; Giziewicz, J.; Gabe, E. J.; Lin, T.-S.; Prusoff, W. H. *Can. J. Chem.* **1987**, 65, 2135.
- (38) (a) Kolodziejek, W.; Klinowski, J. *Chem. Phys. Lett.* **1999**, 303, 183. (b) Swapna, G. V. T.; Jagannadh, B.; Gurjar, M. K.; Kunwar, A. C. *Biochem. Biophys. Res. Commun.* **1989**, 164 (3), 1086.
- (39) (a) Painter, G. R.; Aulabaugh, A. E.; Andrews, C. W. *Biochem. Biophys. Res. Commun.* **1993**, 191 (3), 1166. (b) Painter, G. R.; Andrews, C. W.; Furman, P. A. *Nucleosides Nucleic Acids* **2000**, 19 (1–2), 13.
- (40) Kovacs, T.; Parkanyi, L.; Pelczer, I.; Cervantes-Lee, F.; Pannell, K. H.; Torrence, P. F. *J. Med. Chem.* **1991**, 34 (8), 2595.
- (41) Marquez, V. E.; Ezzitouni, A.; Russ, P.; Siddiqui, M. A.; Ford, H., Jr.; Feldman, R. J.; Mitsuya, H.; George, C.; Barchi, J. J., Jr. *J. Am. Chem. Soc.* **1998**, 120, 2780.
- (42) Yurenko, Y. P.; Zhurakivsky, R. O.; Samijlenko, S. P.; Ghomi, M.; Hovorun, D. M. *Chem. Phys. Lett.* **2007**, 447, 140, and references cited therein.
- (43) Desiraju, G. R.; Steiner, T. *The Weak Hydrogen Bond*; Oxford University Press: New York, 1999.
- (44) Schneider, B.; Berman, H. M. *Biophys. J.* **1995**, 69, 2661.
- (45) Chalikian, T. V.; Sarvazyan, A. P.; Plum, G. E.; Breslauer, K. J. *Biochemistry* **1994**, 33, 2394.
- (46) Shukla, M. K.; Leszczynski, J. *J. Phys. Chem. B* **2008**, 112 (16), 5139.
- (47) He, Y.; Wu, C.; Kong, W. *J. Phys. Chem. A* **2004**, 108, 943.
- (48) Maag, H.; Nelson, J. T.; Rios Steiner, J. L.; Prisbe, E. J. *J. Med. Chem.* **1994**, 37 (4), 431.
- (49) Neidle, S. *Nucleic Acid Structure and Recognition*; Oxford University Press: Oxford, U.K., 2002.